SAND2008-1705C

Experimental Results of Structural Health Monitoring of Wind Turbine Blades*

Mark A. Rumsey† and Joshua Paquette†
Sandia National Laboratories‡, Albuquerque, NM 87185

Jonathan R. White§
Purdue University, West Lafayette, IN 47907-2031

Rudolph J. Werlink**
NASA, Kennedy Space Center, FL 32899

Alan G. Beattie
Physical Acoustics Corporation, Princeton Junction, NJ 08550

Corey W. Pitchford††
Virginia Polytechnic Institute and State University, Blacksburg, VA 24061

Jeroen van Dam‡‡
National Renewable Energy Laboratory, Golden, CO 80401

A 9 meter TX-100 wind turbine blade, developed under a Sandia National Laboratories R&D program, was recently fatigue tested to blade failure at the National Renewable Energy Laboratories, National Wind Technology Center. The fatigue test provided an opportunity to exercise a number of structural health monitoring (SHM) techniques and nondestructive testing (NDT) systems. The SHM systems were provided by teams from NASA Kennedy Space Center, Purdue University and Virginia Tech (VT). The NASA and VT impedance-based SHM systems used separate but similar arrays of Smart Material macro-fiber composite actuators and sensors. Their actuator activation techniques were different. The Purdue SHM setup consisted of several arrays of PCB accelerometers and exercised a variety of passive and active SHM techniques, including virtual and restoring force methods. A commercial off-the-shelf Physical Acoustics Corporation acoustic emission (AE) NDT system gathered blade AE data throughout the test. At a fatigue cycle rate around 1.2 Hertz, and after more than 4,000,000 fatigue cycles, the blade was diagnostically and visibly failing at the blade spar cap termination point at 4.5 meters. For safety reasons, the test was stopped just before the blade completely failed. This paper provides an overview of the SHM and NDT system setups, and some test results.

---

† Members of the Technical Staff, Wind Energy Technology Department, PO Box 5800, Mail Stop 1124, Albuquerque, NM, 87185, www.sandia.gov/wind/

‡ Sandia is a multiprogram laboratory operated by Sandia Corporation, a Lockheed Martin company, for the U.S. Department of Energy under contract DE-AC04-94AL85000.

§ Graduate Research Assistant, Department of Mechanical Engineering, 140 South Martin Jischke Dr., https://engineering.purdue.edu/~white69/

** Lead Project Engineer, 5403 OSB, Mail Stop NEF7

†† Graduate Research Assistant, Center for Intelligent Material Systems and Structures, Department of Mechanical Engineering, 310 Durham Hall, Mail Code 0261, www.cimss.vt.edu/

‡‡ Test Engineer with Windward Engineering (on assignment at NREL/NWTC), Windward Engineering, 10768 S. Covered Bridge Canyon, Spanish Fork, UT 84660, www.windwardengineering.com/

Nomenclature

AE = *Acoustic Emission*
ATLAS = *Accurate Time-Linked Acquisition System*
DAS = *Data Acquisition System*
HP = *High Pressure*
Hz = *Hertz*
KSC = *Kennedy Space Center*
LP = *Low Pressure*
MeV = *Million Electron Volts*
MFC = *Macro-Fiber Composite*
NASA = *National Aeronautics and Space Administration*
NDT = *Nondestructive Testing*
NREL = *National Renewable Energy Laboratory*
NWTC = *National Wind Technology Center*
PAC = *Physical Acoustics Corporation*
PZT = *Piezo-electric Transducer*
RTV = *Room-Temperature Vulcanizing*
SHM = *Structural Health Monitoring*
SNL = *Sandia National Laboratories*
TX = *Twist-Bend Experimental*
UREX = *Universal Resonance Exciter*
VT = *Virginia Tech*

I. Introduction

In 2002, Sandia National Laboratories (SNL) initiated a research and development program to demonstrate the use of carbon fiber in subscale wind turbine blades.[1,2,3] From this effort, SNL created three 9 meter designs with assistance from Global Energy Concepts[4], Dynamic Design Engineering[5], and MDZ Consulting[6]. From each blade design, seven blades (a total of 21 blades) were manufactured by TPI Composites[7,8]. All blades were designed for a 100-kilowatt stall-controlled turbine, a wind turbine SNL utilizes for field testing.[9]

The second blade design, the TX-100 (Twist-bend Experimental), was designed to have passive aerodynamic load reduction by orienting unidirectional carbon fiber at an optimum angle of 20° off the pitch axis in the skins.[10,11,12,13,14,15] The TX-100 blade also contained a fiberglass spar cap that terminated at 4.5 meters, mid-span in the blade. It was determined that the large amount of carbon contained in the skin was adequate to carry loads outboard in this design, making a full-length spar cap unnecessary. A simplified drawing of the planform of the TX-100 blade is shown in Figure 1. The area of the blade skin containing carbon fiber is shown in blue, and the unidirectional fiberglass spar cap is shown in red.

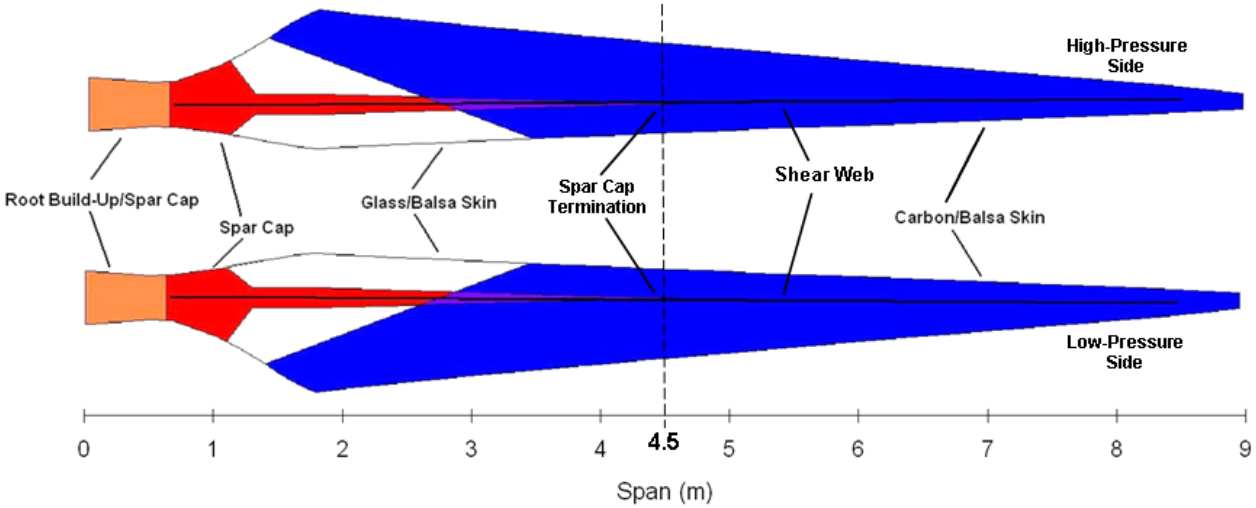

Figure 1 – Diagram showing major structural elements in the TX-100 wind turbine blade.

In support of the SNL blade research and development program, a comprehensive set of tests was defined. The results from a series of static blade tests have already been reported.[16] The particular test described in this paper was a fatigue test of a TX-100 wind turbine blade, to blade failure. The primary goal of the test was to acquire a fatigue dataset that would be used to help validate the blade design and structural computer codes,[17] and to provide feedback in the blade design and manufacturing process. However, fatigue testing a pristine newly manufactured blade over the full life cycle of the blade also provides a unique opportunity to exercise structural health monitoring (SHM) and Nondestructive Testing (NDT) systems in a laboratory environment. The objectives of this fatigue test were to:

1. Determine structural properties of the blade through fatigue testing,
2. Determine fatigue strength and failure mode of the blade,
3. Investigate new sensor technologies for damage detection and structural health monitoring.

II. Structural Health Monitoring Technologies

As utility-size wind turbines increase in size, and correspondingly their initial capital investment cost, there is an increasing need to monitor the health of these structures. Acquiring an early indication of structural or mechanical problems allows operators to better plan for maintenance, possibly operate the machine in a de-rated condition rather than take the turbine off-line, or in the case of an emergency, shut the machine down to avoid further damage.

Numerous damage detection, condition and structural health monitoring devices, techniques and algorithms exist for a whole host of structures.[18,19,20,21,22] This paper, however, will focus on the SHM and NDT techniques that were applied during a fatigue test of the TX-100 wind turbine blade. The specifics of each SHM and NDT technique used will be individually described in the Test Setup section that follows.

III. Test Setup

A. Test Specimen

The test specimen was TX-100 wind turbine blade #002. The blade was 9.0 meters (29.5 feet) long and weighed 160.5 kg (354.0 pounds).

B. Test Location

The fatigue test was performed at the National Wind Technology Center (NWTC)[23], a laboratory within the National Renewable Energy Laboratory (NREL)[24] complex. The NREL headquarters is located in Golden, Colorado. The NWTC is located south of Boulder, Colorado. The blade fatigue testing was performed in the highbay in building A60.

C. Test Fixture Hardware and Blade Structural Loading

The blade was bolted to a 1360 kN-m (1,000 ft-kip) seismic-mass test stand in a cantilever and approximate horizontal orientation with the low-pressure blade surface facing down. Figure 2 shows a photo of the test area.

The fatigue test was planned such that the blade would fail sometime between 1 to 3 million cycles, or over 1 to 2 months of testing. The oscillating load was calculated and prescribed to simulate the cyclical loading that the blades would see in a 20-year field operation, but at an accelerated damage level. The loading was developed by taking into consideration the results of the previously completed static test along with the standard values used to calculate fatigue of the material components of the blade carbon/epoxy and glass/epoxy.[16]

Fatigue cycles were induced in the blade by using a novel resonant system called the Universal Resonance Exciter (UREX). The UREX system consisted of a hydraulically driven mass, weighing 620 kg (1360 lb), mounted approximately at 1.6 meters from the blade root, at approximately maximum blade chord, and an outboard mass weighing 180 kg (390 lb) mounted at the 6.75 meter station. The UREX was driven to excite the first flap frequency and induce a cyclic load in the blade. The applied moment range was controlled by adjusting the frequency and stroke of the UREX. Adjustments were made automatically by the UREX controller based on the feedback signal of an accelerometer that was placed on the blade tip. From time to time manual adjustments were made to the frequency if the blade frequency had changed due to temperature effects. The test frequency varied around 1.2 Hertz (Hz).

All the equipment on the blade (UREX, sensors, actuators, cables) was weighed prior to the fatigue testing. This was the tare load. The mass of the blade was not included in the tare load. A further detailed discussion of the UREX, fatigue test setup, and model validation process can be found in reference 25.

The blade was loaded with a reversal ratio, R=0.1, with the low-pressure down-facing surface in constant compression.[26] For the first 1 million cycles, the maximum load corresponded to a root moment of approximately

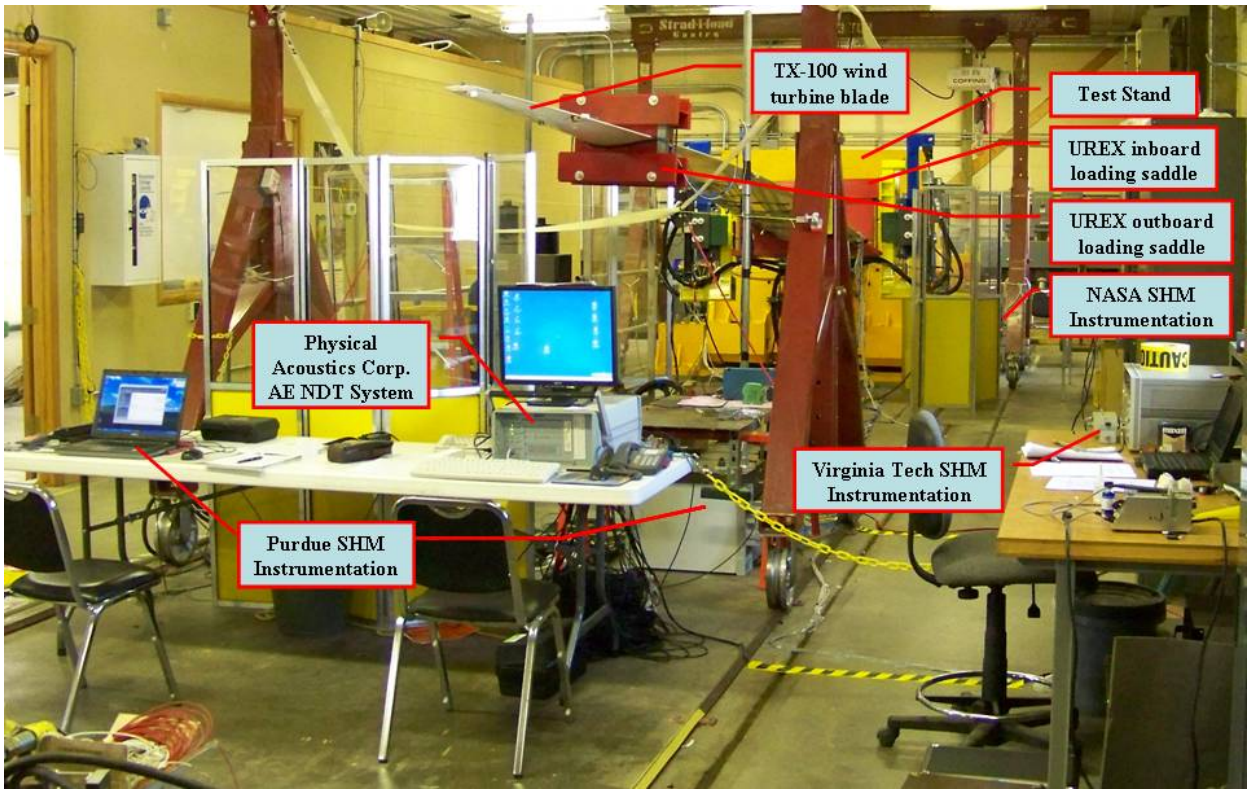

Figure 2 – Photo of the blade fatigue test setup.

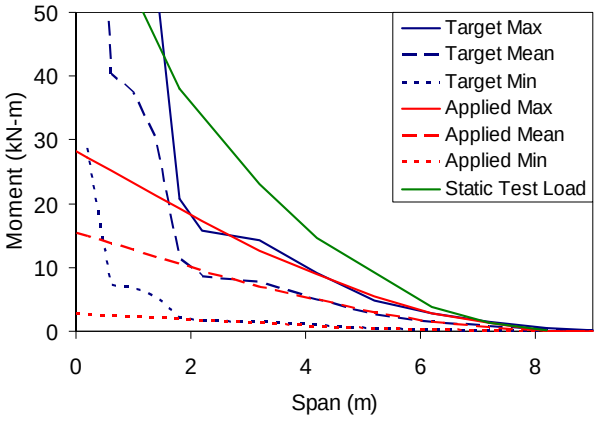

Figure 3 – Calculated UREX fit of 4-million-cycle target load for TX-100 fatigue test.

31% of that which caused failure in the static test. This load level was predicted to cause failure in 4 million cycles. Starting at 1 million cycles, the load was increased in 10% increments and every 500k cycles thereafter. The target and applied test loads for the first load step and the applied test load for the static test are shown in Figure 3.

No load cell was used during the test. Instead a calibration pull was performed on the blade and the strain was measured at the root. The load was then calculated from the strain seen at the root. The output from strain gage G5 (see Figure 4) was connected to a signal conditioner to provide an amplified high-level output signal and was made available to the other test parties as the derived load level.

Ambient temperature near the blade root was continuously measured throughout the test.

D. Possible Blade Failure Mechanism and Location

To strategically place SHM sensors, we needed to know the TX-100 blade failure mechanism in fatigue and the failure location (neither were known). Our only previous experience with this blade design was a TX-100 static test to blade failure, and the blade failed between 1 and 3 meters from the root, near maximum chord, on the compression side. In the previous static test of a TX-100 blade, failure was dominated by structural characteristics rather than material weakness. Furthermore, previous fatigue tests of other similar 9-meter blades have resulted in failure in the transition region of the blade near maximum chord. Using this information, we recommended the SHM sensors be placed around the maximum chord area on the blade. For this test setup, the compression side would be facing down toward the floor.

E. Strain gages

Thirty 1000-ohm metal foil strain gages were installed on the gel-coat surface of the blade in a layout as shown in Figure 4. The strain gages were zeroed at the flapwise tare load. Detailed information about the strain gauge locations and orientations is given in reference 25.

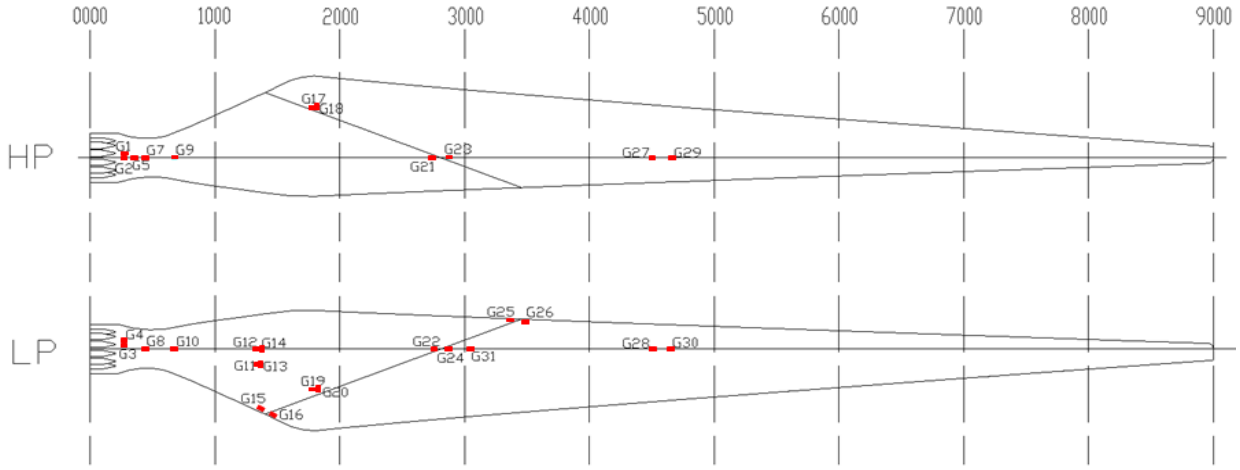

Figure 4 – Diagram showing the layout of strain gages.

F. Physical Acoustics Corporation Acoustic Emission (AE) NDT System

The Physical Acoustics Corporation (PAC) acoustic emission NDT system was setup by Dr. Alan Beattie and Dr. Adrian Pollock.

The acoustic emission sensors specifically monitor sound waves that propagate on the blade surface. These sound waves are often caused by structural damage (that is, fiber breakage, delamination, disbonding) occurring in the blade.

During preliminary tests, acoustic velocity and attenuation measurements were made by placing two PAC AE sensors 0.15 meters apart on a section of a TX blade and doing ten pencil lead breaks 0.05 meters behind each sensor. The vectors between the two sensors were oriented at angle increments of ten degrees from the blade axis. For the frequency response of R6I sensors, the attenuations lay between 0.02 and 0.10 dB/mm. This corresponds to a spread in attenuation of 8 to 40 dB between sensors for the maximum chosen separation of 0.4 meters.

Twenty-four PAC Model R6I AE sensors were mounted on the blade over critical areas and interfaces inside the blade. Because of the diverse material characteristics, orientations and interfaces of the internal components in the blade the acoustic velocity was very anisotropic. The sensor layout shown in Figure 5 was determined on site after the acoustic characteristics had been measured. (Sensor #25 was not used during the fatigue test.)

A PAC DiSP system using PAC AEwin software acquired and processed the AE signals.[27] Much of the data processing was done by custom programs.

After the initial system checkout, NREL testing staff operated the PAC AE NDT system.

G. NASA Kennedy Space Center SHM System

Rudy Werlink, with NASA Kennedy Space Center, implemented an impedance-based SHM technique by instrumenting the blade with an MFC actuator and three sensors on the high-pressure side of the blade, and an MFC actuator and two sensors on the low-pressure side. Both actuators were energized with a random-frequency input signal. Data was collected for 30-seconds in the following sequence of configurations:

1. Up-side array actuated with the blade load not cycling.
2. Up-side array actuated with blade load cycling, and using an electronic filter on the sensor output to reduce the self-generated voltages resulting from the reaction of the blade while resonating.
3. Down-side array actuated with blade load not cycling.
4. Down-side array actuated with blade load cycling, and using the sensor output filter.

His setup was an incremental enhancement, with the application of the electronic filter, to the setup on previous wind turbine blade tests.[28] The Smart Material MFC actuator, model 8557-S1, was 3.375 x 2.25 inch in size. The MFC sensors, model 5-21, were 1.5 x 1 inches in size. The actuator/sensors needed to encompass the expected failure area. Close-up photos of the NASA sensor arrays are shown in Figure 6.

As in the previous tests, NASA provided all their test equipment except the data acquisition system (DAS). Data from the MFC sensors was collected by a SNL ATLAS[29,30,31] at a sample rate of 5,000 Hz. After the initial system checkout, NREL testing staff operated the SNL ATLAS, exercised the NASA SHM system, acquired the data, and posted the data on a secure NREL FTP file server to allow remote file access by the testing partner.

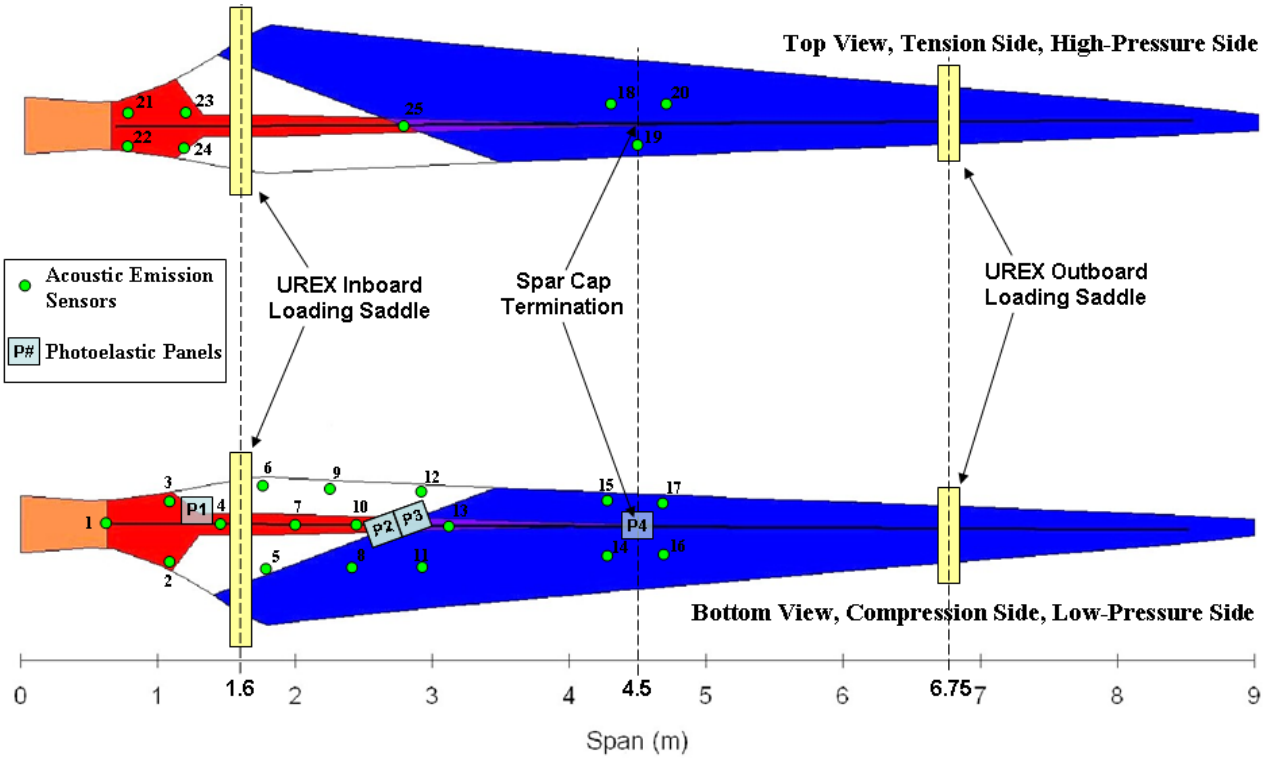

Figure 5 – Layout of the acoustic emission NDT sensors and photoelastic panels.

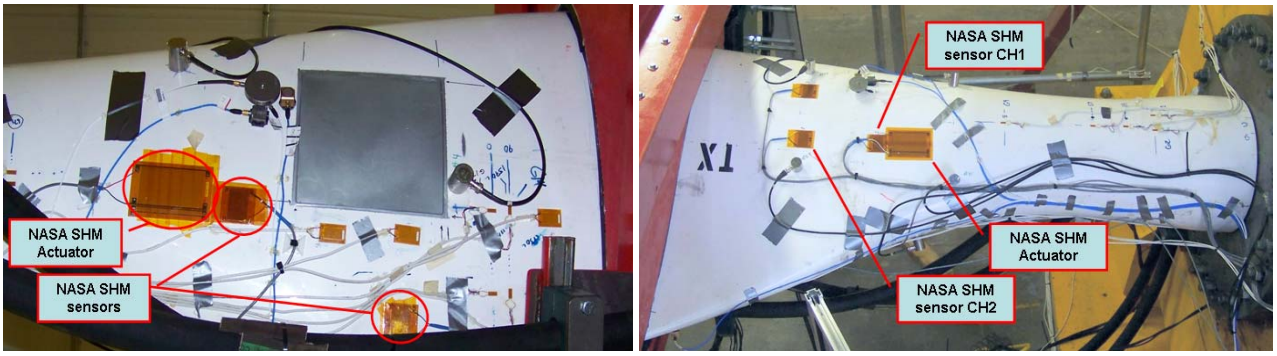

Figure 6 – Photos of the NASA SHM sensor arrays. The left photo shows the low-pressure (downward facing) side of the blade. The right photo shows the high-pressure (upward facing) side of the blade. The larger MFC patches were used as actuators, the smaller MFC patches were used as sensors.

H. Purdue University SHM System

The Purdue University test team was lead by Jonathan White under the guidance of Professor Doug Adams. Purdue provided their test equipment and data acquisition systems, and rotated one to two staff members in and out of the NREL NWTC test site over the duration of the test.

Sensor placement was determined ahead of time using the results from pre-testing on a 15-foot cantilevered helicopter rotor blade recently erected at the Herrick Laboratories at Purdue University.[32] An array of high sensitivity triaxial accelerometers, low-frequency capacitive accelerometers, and piezoelectric actuators with force sensors was distributed over the surface of the blade to monitor the loading and blade damage. A triaxial accelerometer at the tip was used to measure the tip deflection in the flap, lead-lag, and root-tip directions throughout the test. Prior to the start of the fatigue test, a modal analysis of the blade in the flap-wise direction was performed. The SHM approach implemented the restoring force method, a passive structural health monitoring algorithm, using 4-each PCB 3711D1FA20G and 4-each PCB 3711D1FA50G triaxial accelerometers. The method of virtual forces, transmissibility and other time-frequency analysis techniques, active structural health monitoring algorithms, was also applied with 4-each PCB 712A02 actuators, 4-each PCB 208C01 force sensors and 4-each PCB 356B18 triaxial accelerometers. The Purdue test team also recorded passive response measurements throughout the test when the blade was at fatigue load. A few photos of the Purdue SHM setup are shown in Figure 7. More details of the Purdue instrumentation setup are given in reference 33.

Figure 7 – Photos of some of the Purdue SHM instrumentation.

I. Virginia Tech SHM System

The Virginia Tech (VT) test team was lead by Corey Pitchford under the guidance of Professor Dan Inman. The VT impedance-based SHM system consisted of 6-each self-sensing actuators, Smart Material MFC, model M2814-P1, mounted on the blade surface, and an Agilent HP4192A impedance analyzer.[34] The instrumentation setup can be seen in Figure 8. Initially for this test it was desired to use an Analog Devices, Inc., AD5933 Impedance to Digital Converter integrated circuit to measure the impedance. Unfortunately, problems arose getting the AD5933 to produce acceptable real impedance results so an Agilent HP4192A impedance analyzer was used in its place. Preliminary tests back at VT on a CX-100 wind turbine blade section showed that using MFC sensors on the blade in place of PZTs and mounting the MFCs on the outside of the blade instead of the inside caused less structural information to show up in the impedance, but damage was still detected. The HP4192A was shipped to NWTC for the fatigue test, along with a laptop running Piezoelectric Resonance Analysis Program (PRAP) version 2.1 software to control the impedance analyzer and record data. The switchbox (the blue box shown in Figure 8) was built so that all six MFCs could be connected to the impedance analyzer simultaneously, and then one could be selected at a time to be the input. This greatly simplified the routine for collecting impedance data.

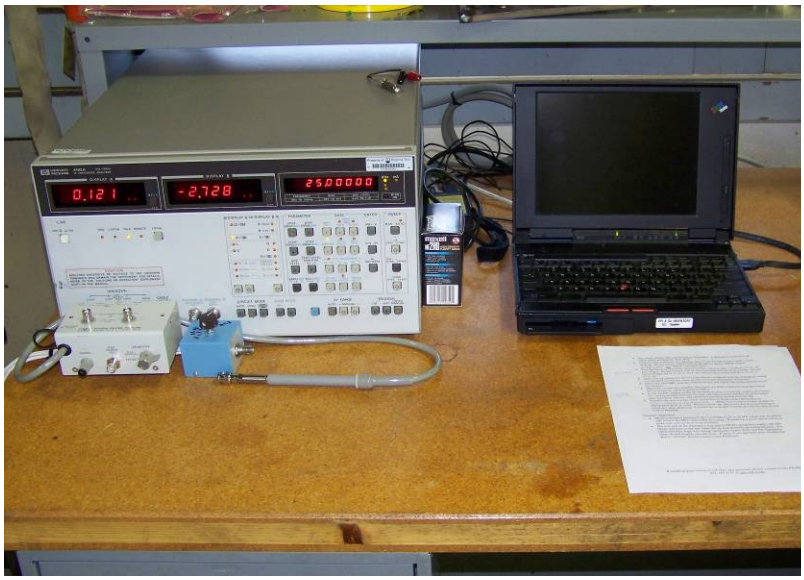

Figure 8 – Setup of the Virginia Tech SHM instrumentaton.

The locations where the MFCs were bonded are all on the low-pressure, downward-facing side of the blade between 1 and 3 meters from the root. Failure was expected in this area from modeling and previous similar tests.[16] The locations within this area were chosen based on the internal geometry of the blade. This geometry along with the sensor locations is illustrated in Figure 9. Figure 10 shows two photos of the MFCs bonded to the wind turbine blade, along with some of the other sensors used on the blade. Failure was expected near the spar cap close to the 1 meter area, so three MFCs were mounted in this area and were named S1, S2, and S3. One additional MFC was mounted on the spar cap region near the intersection of the spar cap, glass/balsa skin, and carbon/balsa skin and was named S4. Finally, two MFCs were mounted on the glass/balsa and carbon/balsa intersection on the skin, one at about 2 meters, GC1, and one near the spar cap, GC2.

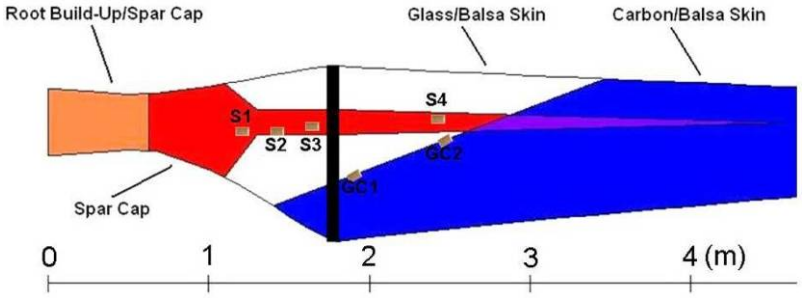

Figure 9 – Diagram showing layout of Virginia Tech sensor array.

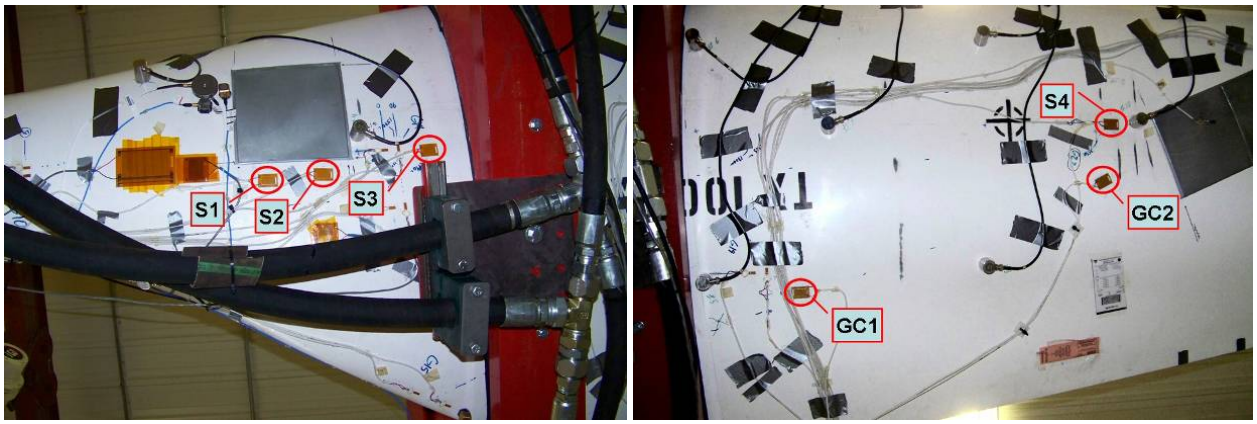

Figure 10 – Photos showing the Virginia Tech SHM sensor arrays. The self-actuating sensors S1, S2, S3, S4, GC1 and GC2 are circled in red.

J. Miscellaneous Instrumentation

Four 8-inch by 8-inch photoelastic panels were applied on the blade surface over key locations in the blade as shown in Figure 5. Three of the four photoelastic panels are visible in the photos shown in Figure 10. The photoelastic panels were used to provide a qualitative evaluation of the load/strain paths.

Two FLIR ThermaCAM infrared (IR) thermography cameras, models P60 and SC640, were used at various times to monitor and obtain snapshots of thermal gradients and hot-spots as the fatigue test progressed.

The photoelastic and IR imagery have not been analyzed and therefore will not be discussed further in this report.

K. Test Procedure

All strain gages on the blade and the ambient temperature near the blade root were monitored continuously throughout the fatigue test. At least once a day the fatigue test was stopped by halting the UREX to acquire datasets for the NASA, Purdue and VT SHM systems, and to inspect the blade for any damage. Each SHM diagnostic system was exercised in sequence to avoid signal interferences. Periodically, the NREL testing staff would post test data, photos and log files on a secure NREL FTP file server to allow remote file access by the testing partners.

IV. Results

The TX-100 blade fatigue test started on July 19, 2007, and ended October 23, 2007, at 4,001,558 fatigue cycles. Starting at about 700,000 cycles, the blade developed a multitude of gel-coat cracks, first parallel to the span axis and then parallel to the chord axis, between 2.0 meters and 2.5 meters. At about 2.5 million cycles, a larger visible crack developed parallel to the chord axis on the high-pressure (upward-facing) side, near the 4.5 meter station. The crack then grew along the 20º off-pitch-axis carbon fiber direction until the test was stopped at 4 million cycles. Figure 11 shows the high-pressure (upward facing) surface damage above the spar cap skin interface.

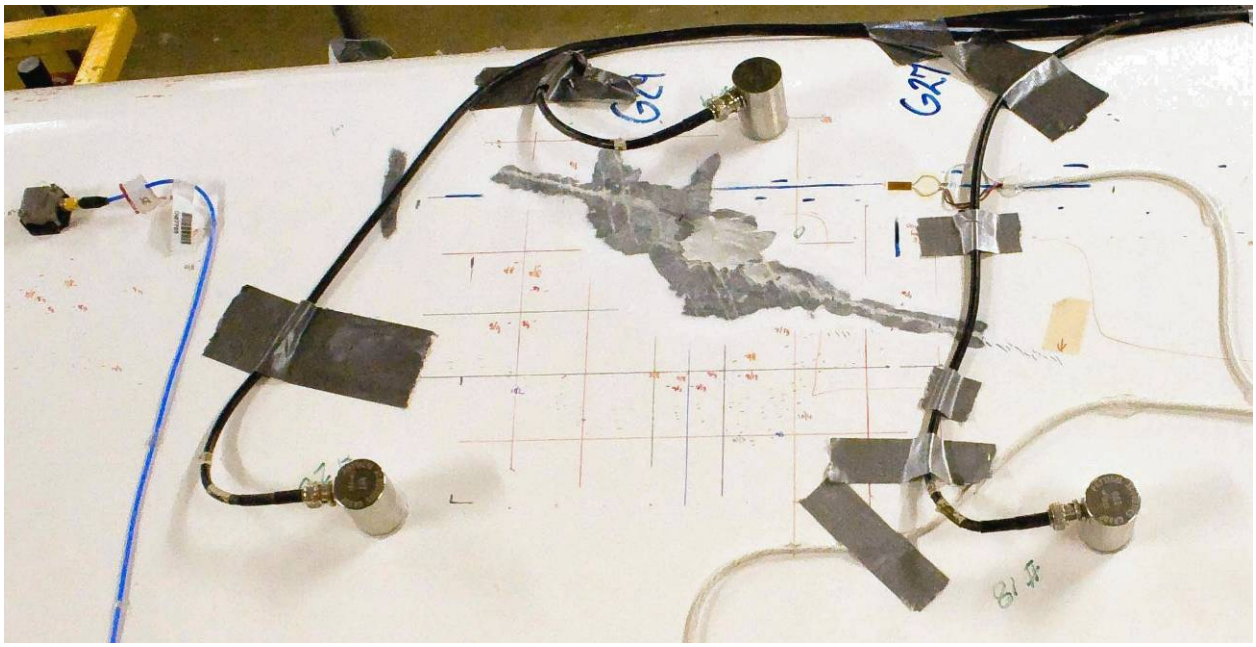

Figure 11 – Photo showing the blade surface around the area of failure. Some of the gel-coat has been manually removed to better evaluate the underlying damage.

Soon after the fatigue test started, the PAC AE NDT system received significant AE events and then clearly followed the evolution of blade failure. The acoustic emission data showed damage accumulating on the high-pressure upward-facing surface around the end of the spar cap at 4.5 meters, with no significant damage in any of the other monitored areas. Significant damage did not appear until about 3.55 million cycles and extreme damage started at 3.78 million cycles. Compare the AE events shown in Figure 12 to the visual damage shown in Figure 11.

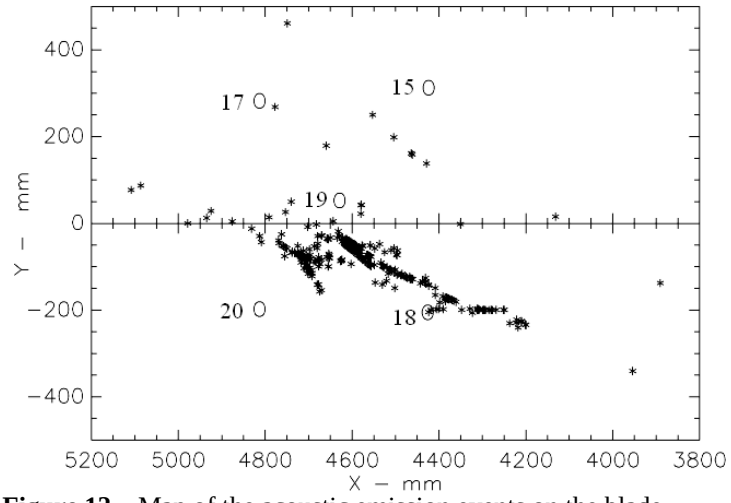

Figure 12 – Map of the acoustic emission events on the blade.

The parameter used to indicate damage was a measure of the detected acoustic energy emitted per cycle in the damaged region. To determine the intensity of the emission, the true energy of the waveforms was used. Once the waveform was digitized, the true energy was easy to measure. It is simply the sum of the product of the square of each digitized voltage times the digitization interval over the entire length of the transient signal. Knowing the input impedance of the preamplifier allows the calculation of the energy. In PAC DiSP energy units, the calibration of N units is E = Nx0.000931 milli-attoJoules or E = $Nx6.7041x10^{-6}$ MeV. The rate of generation of acoustic energy can be obtained from the slope of the summed energy versus time curves. Knowing the frequency of blade cycling gives

the acoustic energy generation rate in MeV/cycle. For most of the test, this rate was less than 0.01-MeV per cycle. At the point of peak damage, this rate went up to 30 MeV per cycle. See Figure 13 and Figure 14.

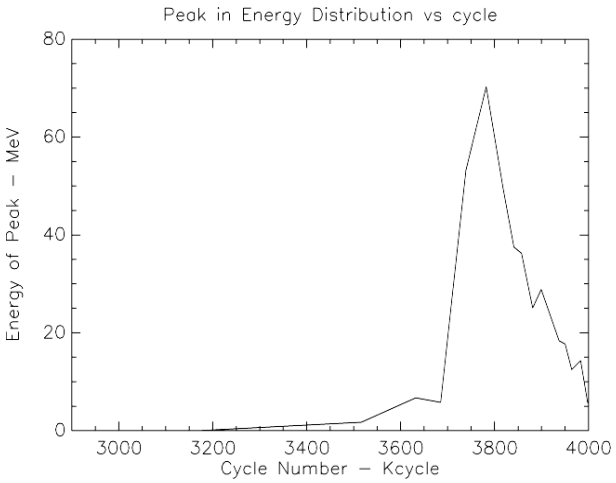

Figure 13 – Peak acoustic emission energy versus cycle count.

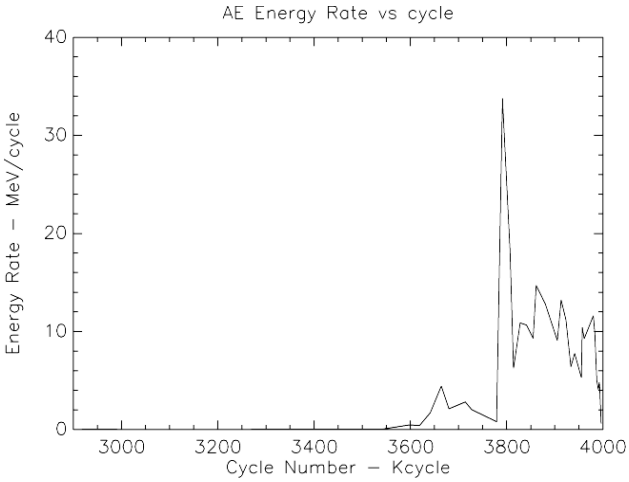

Figure 14 – Acoustic emission energy rate versus cycle count.

The NASA SHM system was placed entirely in-board from the maximum blade chord. This was the location where the blade had failed previously in static testing.[16] However, and unfortunately, this was not where the blade failed in fatigue.

The strains placed on the MFC sensors as the blade was loaded from the UREX mass and the blade movement may have blocked the random input signals from the actuators causing erroneous sensor data. All this resulted in noisy data. However, the analysis to date suggests that the effects of the blade deterioration did affect the boundary conditions enough for sensors CH1 and CH2 to show trends as shown in Figure 15 and Figure 16. The SHM data taken while the blade was cycling has not been analyzed.

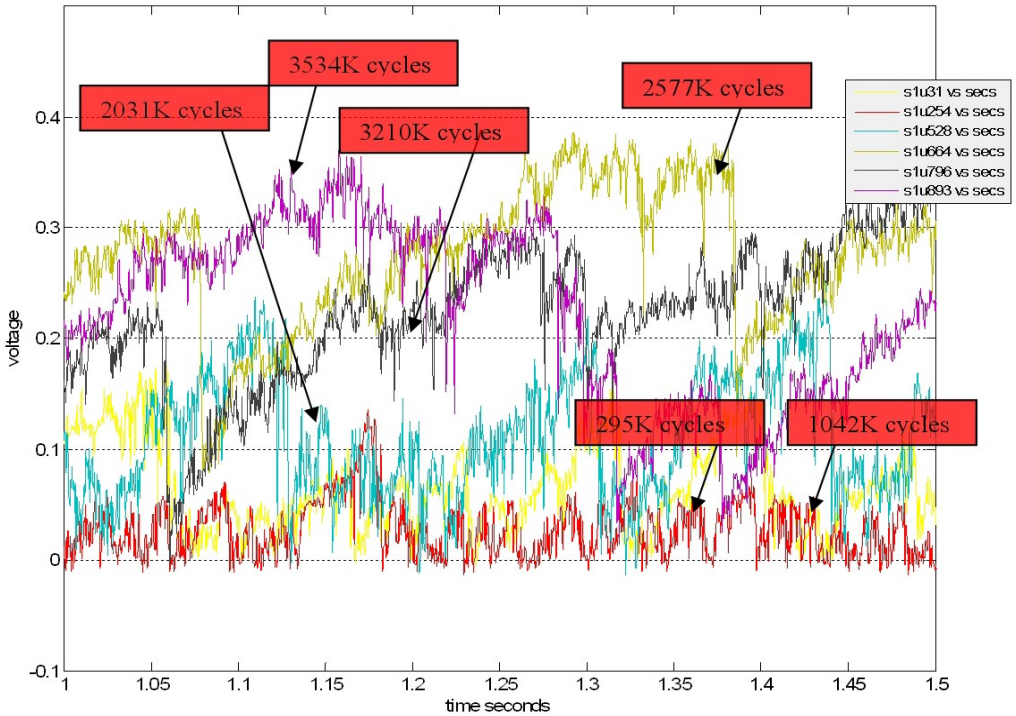

Figure 15 – Plots showing the increase in CH1 response as the fatigue cycles increased from 295 kilocycles to 3,534 kilocycles.

That the sensors showed a trend is very encouraging and with improvements to the system and testing methods, and closer placement of the sensors to the failure area, the NASA SHM system appears viable. NASA will perform the data analysis and report the results of the SHM measurements at a later date.

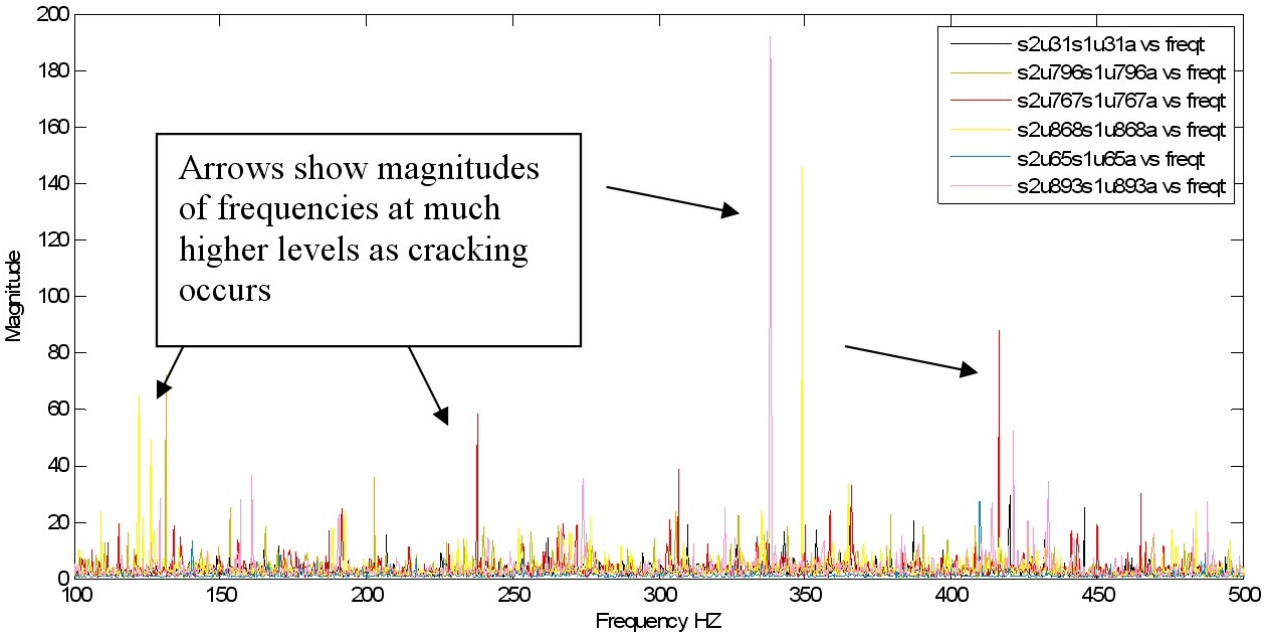

Figure 16 – Plots showing the random input frequency response function for CH2/CH1 showing higher magnitudes as cracking progresses.

The Purdue SHM system did have damage detection sensors; however, none of the sensors were within 2 meters of the failed location. Summarizing the Purdue analysis to date, the in-plane displacement measurements between the damage and root were found to be sensitive to the crack growth and direction.[33] The dynamic features of the rotor blade were sensitive to the variation in ambient temperature. Active diagnostics with the method of virtual forces was sensitive to the damage for in-plane measurements following adjustment for thermal effects (see Figure 17). Impact identification was demonstrated with 93% accuracy of the location and within 1.3% accuracy of the magnitude.

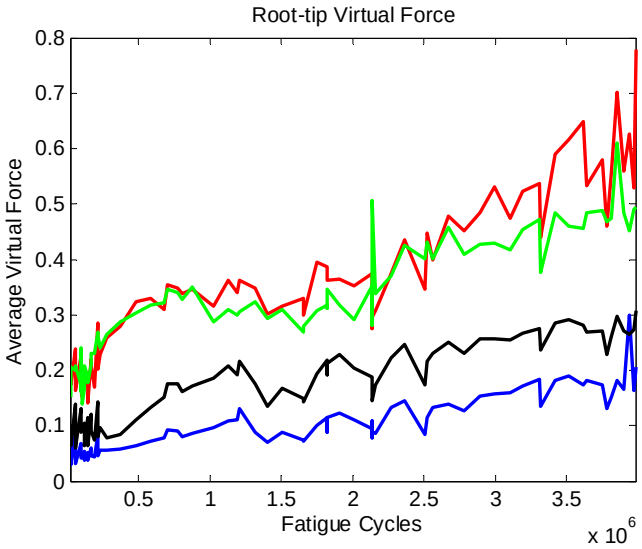

Figure 17 – Root-tip virtual force throughout the fatigue test.

Modal decomposition was an accurate prediction of the excitation mode shapes throughout the test and a practical approach for near-real time load monitoring. Second order harmonics excited by the fatigue system were shown to be on the magnitude of the driving frequency at the tip in the lead-lag and root-tip direction (see Figure 18 and Figure 19). Findings of this test will be instrumental in future development of accelerometer-based wind turbine rotor blade monitoring.

More details of the Purdue analysis are given in reference 33.

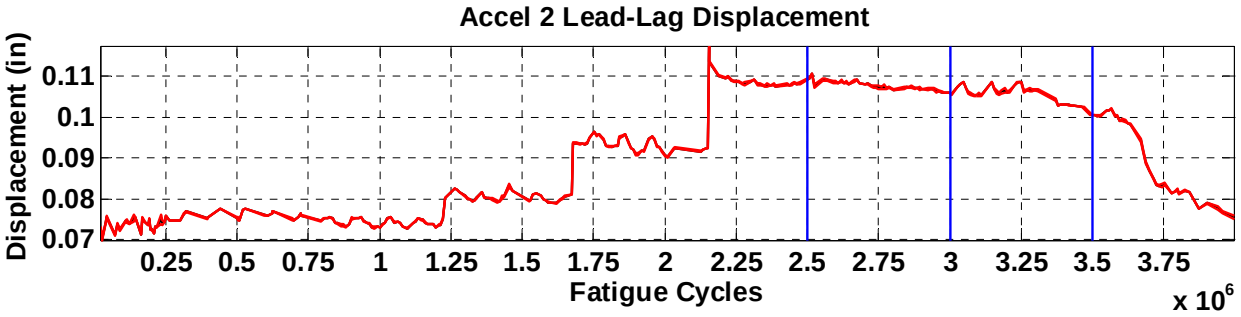

Figure 18 – The blade lead-lag (edge) displacement thoughout the fatigue test.

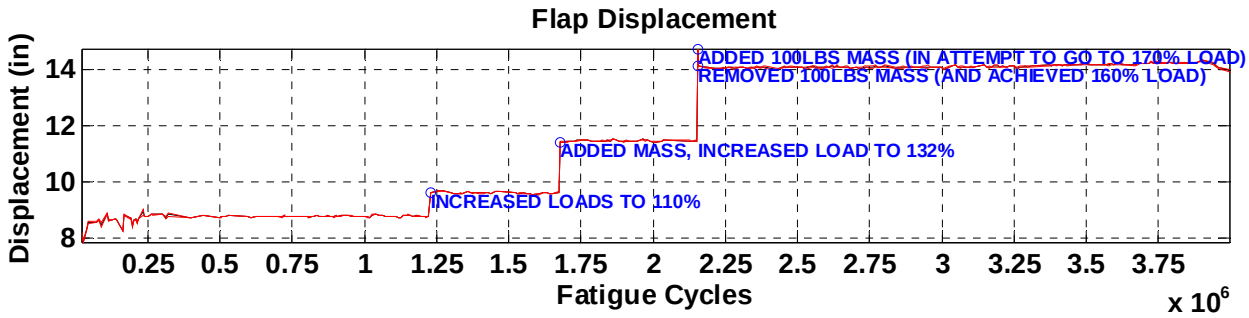

Figure 19 – Calculated blade tip displacement during the fatigue test.

Baseline readings of the VT MFC sensors before the fatigue test started showed no peaks and therefore no structural information from 5 k to 60 kHz. However, recording continued throughout the fatigue test, but as expected from the initial baselines, no damage was detected. These results are disappointing considering that VT's impedance-based SHM system showed the ability to detect damage on the initial tests on a CX-100 wind turbine blade section. However, on the TX-100 blade during the fatigue test the method was insensitive to damage. This is possibly due to the combination of several reasons: using MFC instead of PZT sensors, mounting the sensors on the outside of the blade instead of inside the blade, and likely that the full blade was larger, more massive, and not merely a section and therefore has no boundaries close to the MFC sensors.

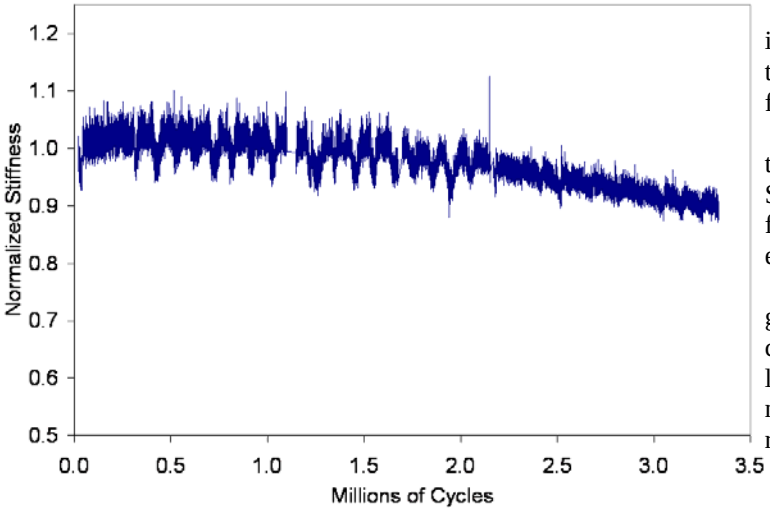

Figure 20 – Response of strain gage G30 versus fatigue cycle count.

The VT SHM system could not record impedances during operation of the fatigue test because the load actuation caused a beat frequency to develop in the impedance data.

The VT SHM system was placed around the maximum blade chord area. The VT SHM system was not close to the area that failed, and therefore was inadequately exercised.

Figure 20 shows the response of strain gage G30 as a function of the fatigue cycle count. The blade can be seen to soften at this location as the cycle count increases. For more information on the strain gage dataset, refer to reference 25.

All the datasets obtained from this fatigue test have not been fully analyzed; further results will be forthcoming.

V. Conclusion

Filtering SHM input signals from background interference still remains a challenge. There was cross-talk interference from other operating active SHM systems and from the cyclic loading of the structure.

The diversity of materials in a composite wind turbine blade provides challenging acoustic properties for AE NDT. Acoustic energy attenuation is comparatively high resulting in sensor separation of 0.4 meters or less, and the acoustic velocities were highly anisotropic.

To date there has been a static and a fatigue test, both to blade failures, performed on two TX-100 blades. The blade failure area in fatigue was significantly different from the blade failure area as a result of the destructive static load.

Structural health monitoring holds promise for future wind turbine applications. However, much work remains to be done in the determination of which technologies are best suited for wind turbine applications, how the technology should be incorporated in the structure in a reliable and cost-effective manner, and how to most effectively use the information that such devices produce to make decisions that impact turbine operation.

Acknowledgments

The lead authors would like to acknowledge and thank the U.S. Department of Energy for its support of blade sensor development programs. We would also like to acknowledge Scott Hughes, Jeroen van Dam and Mike Jenks at the NREL/NWTC blade testing facility for their unwavering professionalism; Alan Beattie and Adrian Pollock with PAC for providing the AE NDT expertise; Jonathan White and Professor Doug Adams with Purdue University for exercising the accelerometry-based SHM techniques; Corey Pitchford and Professor Dan Inman with Virginia Tech for exercising their impedance-based SHM technique; and Rudy Werlink with NASA KSC for exercising his impedance-based SHM technique.

References

1 C.-H. Ong and S. W. Tsai, “The Use of Carbon Fibers in Wind Turbine Blade Design: A SERI-8 Blade Example,” SAND2000-0478, Sandia National Laboratories Contractor Report, March 2000.

2 Ashwill, T, and Laird, D, “Concepts to Facilitate Very Large Blades,” Proceedings, ASME/AIAA Wind Energy Symposium, Reno, NV, 2007.

3 Berry, Derek and Lockard, S., “Innovative Design Approaches for Large Wind Turbine Blades Final Report,” SAND2004-0074, Sandia National Laboratories, Albuquerque, NM, May 2004.

4 Global Energy Concepts, LLC, 1809 7th Avenue, Suite 900, Seattle, WA 98101, (206) 387-4200.

5 Dynamic Design Engineering, Inc., 123 C St., Davis CA, (530) 753-7961.

6 MDZ Consulting, 601 Clear Lake Road, Clear Lake Shores, Texas 77565, (713) 334-5681.

7 TPI Composites, Inc., 373 Market Street, P.O. Box 328, Warren, RI 02885-0367, (401) 247-4010.

8 Berry, D., “Design of 9-meter Carbon-Fiberglass Prototype Blades: CX-100 and TX-100,” SAND2007-0201, Sandia National Laboratories, Albuquerque, NM, September 2007.

9 Jones, P.L.; Sutherland, H.J., Neal, B.A., “LIST/BMI Turbines Instrumentation and Infrastructure**,”** SAND2001-1642, Sandia National Laboratories, Albuquerque, NM, June 2001. http://infoserve.library.sandia.gov/sand_doc/2001/011642.pdf

10 P. S. Veers, G. Bir and D. W. Lobitz, "Aeroelastic Tailoring in Wind-Turbine Blade Applications," Proceedings, Windpower '98 Meeting, pp. 291-304.

11 Lobitz, D. and Veers, P., “Aeroelastic Behavior of Twist-coupled HAWT Blades,” ASME/AIAA Wind Energy Symposium, Reno, NV, 1998, pp. 75-83.

12 Lobitz, D. and Laino, D., “Load Mitigation with Twist-coupled HAWT Blades,” ASME/AIAA Wind Energy Symposium, Reno, NV, 1999, pp. 124-134.

13 D. Lobitz, P. S. Veers and D. J. Laino, “Performance of Twist-Coupled Blades on Variable Speed Rotors,” Proceedings, ASME/AIAA Wind Energy Symposium, Reno, NV, 2000, pp. 404-412.

14 D. W. Lobitz et al., “The Use of Twist-Coupled Blades to Enhance the Performance of Horizontal Axis Wind Turbines,” SAND2001-1303, May 2001.

15 D. Griffin, “Evaluation of Design Concepts for Adaptive Wind Turbine Blades,” SAND2002-2424, Sandia National Laboratories Contractor Report, August 2002.

16 Paquette, Joshua; van Dam, Jeroen; Hughes, Scott, “Structural Testing of 9 m Carbon Fiber Wind Turbine Research Blades,” AIAA-2007-816, *45th AIAA Aerospace Sciences Meeting and Exhibit*, Reno, NV, 2007.

17 Paquette, J; Griffith, D.T., “Development of Validated Blade Structural Models,” AIAA-2008-1297, *46th AIAA Aerospace Sciences Meeting and Exhibit*, Reno, NV, 2008. (to be published)
18 Sutherland, H.J.; Musial, W., "The Application of Non-Destructive Techniques to the Testing of a Wind Turbine Blade" Proceedings, *WindPower 93*, AWEA, Washington, D.C., 1993.
19 Sutherland, H.; Beattie, A.; Hansche, B.; Musial, W.; Alread, J.; Johnson, J. and Summers, M., "The Application Of Non-Destructive Techniques to the Testing of a Wind Turbine Blade," SAND93-1380, Sandia National Laboratories, Albuquerque, NM, June 1994. http://infoserve.library.sandia.gov/sand_doc/1993/931380.pdf
20 James, George, "Development of Structural Health Monitoring Techniques using Dynamics Testing," SAND96-0810, Sandia National Laboratories, Albuquerque, NM, March 1996. http://infoserve.library.sandia.gov/sand_doc/1996/960810.pdf
21 Sundaresan, M.J.; Schulz, M.J.; and Ghoshal, A., “Structural Health Monitoring Static Test of a Wind Turbine Blade,” NREL/SR-500-28719, North Carolina A&T State University Report for NREL, Golden, CO, March 2002.
22 Farrar, Charles R.; Worden, Keith; Todd, Michael D. ; Park, Gyuhae; Nichols, Jonathon; Adams, Douglas E.; Bement, Matthew T.; Farinholt, Kevin “Nonlinear System Identification for Damage Detection,” LA-14353, Los Alamos National Laboratories, Los Alamos, NM, November 2007. http://www.lanl.gov/projects/ei/pdf_files/LA_14353_NonlinearReport.pdf
23 National Wind Technology Center, http://www.nrel.gov/wind/
24 National Renewable Energy Laboratory, http://www.nrel.gov/
25 Paquette, Joshua; Hughes, Scott; van Dam, Jeroen; Johnson, Jay, “Fatigue Testing of 9 m Carbon Fiber Wind Turbine Research Blades,” AIAA-2008-1350, *46th AIAA Aerospace Sciences Meeting and Exhibit*, Reno, NV, 2008. (to be published)
26 Sutherland, H.J., "On the Fatigue Analysis of Wind Turbines," SAND99-0089, Sandia National Laboratories, Albuquerque, NM, June 1999. http://www.prod.sandia.gov/cgi-bin/techlib/access-control.pl/1999/990089.pdf
27 Physical Acoustics Corp., 195 Clarksville Road Princeton Jct, NJ 08550, 609-716-4000, http://www.pacndt.com/
28 Zayas, Jose R.; Paquette, Joshua; Werlink, Rudolph J., “Evaluation of NASA PZT Sensor/Actuator for Structural Health Monitoring of a Wind Turbine Blade,” Conference paper AIAA 2007-1020, 45th AIAA Aerospace Sciences Meeting and Exhibit, Reno, NV, 2007.
29 Berg, D.E.; Rumsey, M.A.; and Zayas, J.R., “Hardware and Software Developments for the Accurate Time-Linked Data Acquisition System”, *2000 ASME Wind Energy Symposium*, 2000, p. 306.
30 Berg, D.E., and Zayas, J.R., “Accurate Time-Linked Data Acquisition System Field Deployment and Operational Experience”, *2001 ASME Wind Energy Symposium*, 2001, p. 153.
31 Zayas, J.; P. Jones, J.; Ortiz-Moyet, “Accurate GPS Time-Linked Data Acquisition System (ATLAS II) User’s Manual”, SAND2004-0481, Sandia National Laboratories, Albuquerque, NM, February 2004. http://www.prod.sandia.gov/cgi-bin/techlib/access-control.pl/2004/040481.pdf.
32 Ray W. Herrick Laboratories, School of Mechanical Engineering, Purdue University, https://engineering.purdue.edu/Herrick/index.html.
33 White, J.; Adams, D.; Rumsey, M.; van Dam, J.; Hughes, S., “Impact, Loading and Damage Detection in Carbon Composite TX-100 Wind Turbine Rotor Blade,” AIAA-2008-1349, *46th AIAA Aerospace Sciences Meeting and Exhibit*, Reno, NV, 2008. (to be published)
34 Pitchford, Corey, “Impedance-Based Structural Health Monitoring of Wind Turbine Blades,” Master’s Thesis, [Aug. 31, 2007]. http://scholar.lib.vt.edu/theses/available/etd-09062007-140545/